Experimental-Numerical Method for Identification of Weighting Function in Preisach Model for Ferromagnetic Materials

Jakub Eichler, Miroslav Novák, Miloslav Košek

Department of Mechatronics and Applied Informatics, Faculty of Mechatronics,
Technical University in Liberec,
Studentská 2, CZ-46117 Liberec 1, Czech Republic
jakub.eichler@tul.cz

Abstract–**The Preisach model weighting function is given by partial derivations of a measured magnetic flux density that leads to high errors. Therefore other methods of the weighing function estimation are used frequently. In order to verify the direct approach the extended experiment was made and data were numerically processed to reduce known errors. It results in model of the hysteresis loop usable in a technical research. The possible errors reduction and further improvements are discussed and recommended.**

Keywords-Ferromagnetics, Preisach model, weighting function, first order revese curve, FORC, data processing

I. Introduction

In present time an advanced experimental technique and extreme computational power of a standard computer allows making and using of models in almost all areas of the electrical engineering and electronics. Suitable model allows a detailed analysis, an optimization, reveals evident errors and makes possible to skip some steps in the realization, which results in the saving of development time and money.

Ferromagnetic materials exhibit very complicated characteristics: strong nonlinearity and the hysteresis. Therefore, the linear model does not represent a device satisfactory. For instance, in the linear model the transformer inrush current after switching of the device into the AC network can reach maximally two times of the steady state value. The real device exhibits the inrush current that exceeds the steady state value 50 times. Therefore, the more exact models of ferromagnetic materials are necessary.

If we consider only the nonlinearity in the ferromagnetic materials, a lot of models can be found in the standard monographs. However, only few models exist for the hysteresis. One of them is well-known Preisach model [1, 2]. While the nonlinear model is one-dimensional, the hysteresis model is two-dimensional (2D), which explains its complexity and difficulty of the use.

The basic of the Preisach model is the weighting function that must be determined from an experiment. Usually the weighing function is made by the trials and error method from the hysteresis loop with the maximal excitation [3, 4], for instance. The agreement with the experiment is limited due to the limited information in the measured data. In principle much better result can be achieved from the extended systematic experiment. The limitation of this natural way is the numerical derivation. Irrespective of the limitation we made a lot of systematic experiments. The data were numerically processed to reduce experimental errors and the numeric derivation was applied to the numerically improved data. Some key results are presented in the paper.

II. Theory

The complete theory of the Preisach model is given in [1]. The theory necessary to understand the paper is in [5], for instance. The Preisach model consists of the small ideal magnetic dipoles having the rectangular hysteresis loop that are systematically arranged in the upper triangle part of a matrix. The matrix lower part has no dipoles. The position of individual dipole in the matrix element is determined by its levels of magnetic field strength H_u that switches the dipole into the up direction and H_d for the switching into the down direction. When the external magnetic field increases, all dipoles under the field horizontal level H_u are switched into the up direction. If the external magnetic field decreases, all dipoles in the right hand part of the magnetic field strength H_d are switched down. The total magnetic momentum of the material is the sum of all individual momentums. Since the increasing magnetic field is represented by the moving of the horizontal line and the decreasing field by the running of the vertical line, the hysteresis is ensured.

The magnetic material properties are given by the 2D weighting function that must be determined experimentally. Since the standard demagnetized state in not well defined [1], the experiment starts with negative saturation. Then the exciting current of the increasing amplitude is applied and the partial hysteresis curves are measured. The points for the equidistant excitation in their decreasing parts are systematically arranged in the dipole net. The weighting function is found by the partial derivation by both the increasing and the decreasing magnetic field strengths H_u and H_d. To reduce high error of the numeric derivation of experimental data, careful

experiment and the sophisticated data processing are necessary to get acceptable results.

III. EXPERIMENT

The experiment differs from standard one in several ways. The initial state is very near the negative saturation, since it is well-defined. The excitation is made by the harmonic current source in agreement with the basic theory. Its frequency is very low. We were using 1 Hz in order to reduce the effect of the eddy currents.

The scheme of the apparatus is in Fig. 1. The current source is made from the programmable voltage source PS by adding high resistances R_1 and R_2 that have negligible inductance. The condenser C is used for the filtering of noise coming from the programmable source. A core of the toroid transformer Tr is made from the tested material. The exciting harmonic current is derived from the voltage V_c and the response, the secondary voltage, is measured by another voltmeter V_{sec}.

The measured specimen is made from a standard grain oriented M130 laminated steel of 0.3 mm thickness. The core diameters are $D = 220$ mm and $d = 160$ mm and depth $h = 30$ mm. The primary winding has $n_p = 100$ turns and for the secondary $n_s = 300$.

The measurement is fully automated by the control program written in MATLAB that controls namely the programmable source Kikusui PCR 2000 LA. Both the voltages were measured by the ADC cards NI USB 6212. Alternatively, two ADC cards are used simultaneously, in order to avoid the crosstalk between channels in case of using only one card.

The current waveform started from the negative DC current, followed by two harmonic periods, see Fig. 4 later. The amplitude of the periodic part gradually increases for each attempt. The ADC sampling time is 5 µs. Total 1800 waveforms were measured from magnetic field strength $H = -650$ A/m to $H = 650$ A/m. Therefore, the amplitude step of the magnetic field strength was very small – circa 0.7 A/m.

The current waveform should be harmonic. It is valid, when its maximum is negative. Small deviations from harmonic shape take a place when the primary current crosses zero values, as it is presented in Fig. 2. The explanation is in Fig. 3 where both the current difference from harmonic waveform and the induced secondary voltage are present. For easy comparison the current deviation changes the sign and both the curves are normalized to negative minimum. A good similarity is evident for peaks. It can be used for the current improvement by simple way. Outside peaks the improvement is more complicated, but it does not seem to be necessary.
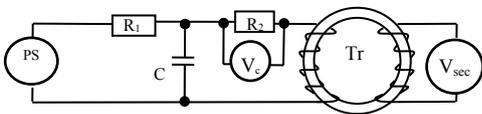

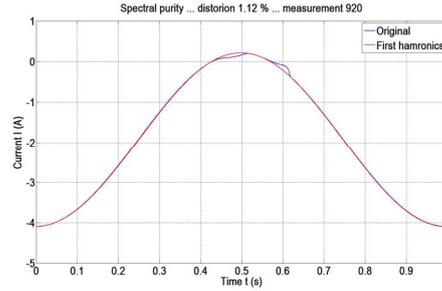Figure 1. Electrical scheme of apparatus.

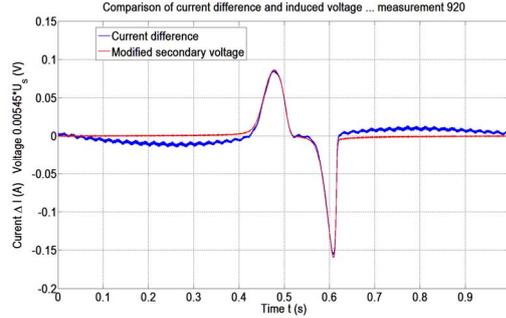Figure 2. Current waveform deviation from pure harmonics.

Figure 3. Effect of secondary voltage to primary current.

IV. DATA PROCESING

In order to reduce the experimental errors, especially at low excitations, the data saved in the numeric files are processed in several steps:

- Waveform is withdrawn from the file;
- Noise is reduced and data smoothed;
- The output voltage drift is eliminated;
- Exciting current and response magnetic flux waveforms are synchronized;
- The output waveform order can be changed.

The measured waveforms are in Fig. 4. Total time of one measurement is 10 sec while the waveform needs only 2 sec and its position is random. The waveform detection and taking out is necessary.

The waveform detection can be made by several means. The increase above the predicted trigger level is the simplest but also the worst solution. We used the parasitic properties of the voltage source. When starting the sinusoidal part of the current waveform, short negative current pulse appears, see the upper part of Fig. 4. On the transformer secondary the voltage pulse is found, see the lower part of Fig. 4. Also, the detection marks are present in Fig. 4. The details of pulses are in following Fig. 5. Note that the voltage and current waveform are not synchronized in the case of two ADC cards use.
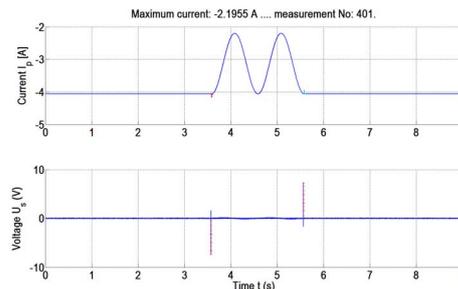

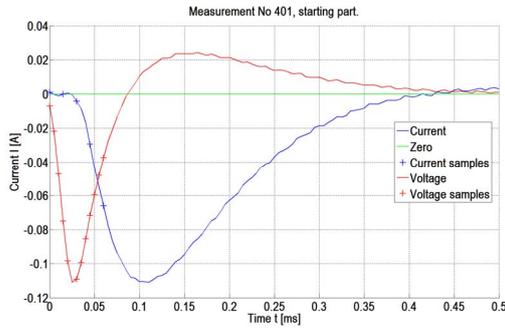Figure 4. Current and voltage waveform detection.

Figure 5. Current and voltage pulses after staring the waveform.

Figure 6. Filtering of the secondary voltage by FFT filter[1].

Both the current and the voltage pulses are used for finding the start of excitation and the signal synchronization. As for current, the edge is found by the comparison of the current samples with distance of 50 µs, which can be changed. If there is high difference and the difference is confirmed for the following two pairs, the beginning of the periodic part of current waveform is detected. It is illustrated also in Fig. 5. Since the current stabilization (the slow increase after the edge in Fig. 5) is not caused by the magnetic properties of the sample, this part in the length of about 300 µs is withdrawn from the waveform.

The simplest way to detect the start of the voltage waveform is to detect the minimal negative voltage, see lower part of Fig. 4. It is possible for low excitations only. In the case of high excitation the useful voltage waveform should be detected. Reliable procedure of the edge finding must be applied. It is similar to that for current edge and the details are in Fig. 5 for voltage waveform.

The similar procedure is applied for finding the end of the periodic part of the waveforms. Also the time of the period can be used, since it is known with high accuracy. If only one card is used the start of the current waveform is enough and the voltage waveform can be used for the check.

If two independent ADC cards are used, the start of both the current and the voltage must be found in order to synchronize waveforms. The synchronization shift can be found from voltage and current edge shift, as in Fig. 5. Fig. 5 confirms the synchronization of about 50 µs for the parameters used in the MATLAB script.

The second step of the data processing is to apply filter to both the waveforms in order to eliminate the noise. In MATLAB, there are many possibilities, e.g. the running average, FIR filtering, FFT filtering, median filtering. The running average can be made by the user function, the built-in function *filter* or the external function *savitzkyGolayFilt* [6, 7]. We have found that the last choice was the best one as for the running average.

The FFT filtering applies an ideal low-pass filter to the spectrum obtained by FFT and performs the inverse FFT. Its application is very simple, but the understanding the spectrum features is necessary. The advantage of the FFT filtering is a very high speed; the filtering may be hundred times faster than the filtering
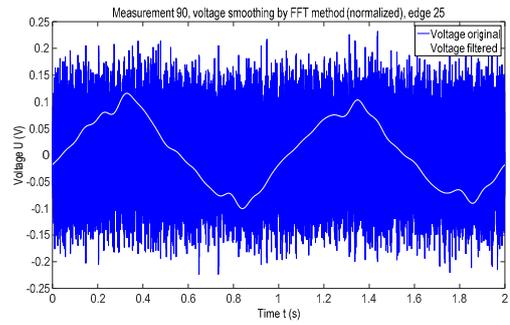
using the function *savitzkyGolayFilt.* On the other hand, the use of the ideal filter can lead to the well-known Gibbs effect. In special cases the filtered signal can be systematically damaged in the starting and finishing parts. An example of the secondary voltage filtering is shown in Fig. 6. The same result can be achieved by the function *savitzkyGolayFilt,* but the time is two orders higher.

The FFT filtering is a non-linear operation. It must be taken into account if we use the integration and the filtering of the secondary voltage. Both operations work as filters, but the integration must be applied as the last operation. The numeric integration of the secondary voltage is included into filtering. The output of filtering operation is the smoothed current and smoothed magnetic flux.

Since the magnetic flux is obtained by the numeric integration of the secondary voltage, one difficulty appears. The integration is followed by drift due to the presence of a small and almost constant component in the integrated function. It is important especially in low current amplitudes, when the excitation magnetic field almost fully saturates the sample. The drift can be reduced by following steps. First, linear function derived from the first and central magnetic flux waveform minimums is subtracted from waveform. Then both the minimums of corrected waveform are the same. The procedure is repeated for central and last minimum and, finally, for both the maximums. The result is shown in Fig. 7. Since the magnetic flux can contain any constant, it is normalized to zero minimum in Fig. 7.

Other method is to reduce the offset voltage prior the integration. We can calculate the offset in the beginning part of the signal where the voltage is constant; see lower part of Fig. 4, for instance.
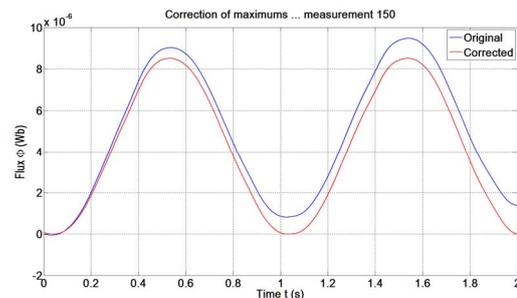

Figure 7. Elimination of the drift for low excitation.

[1] In order to see details, both the waveforms in Fig. 6 are normalized to have maximum and its half.

In the ideal case of no loss magnetic material the current and the magnetic flux maximums are in the same time. It is especially valid for low excitations, when the magnetic flux waveform is close to harmonic one. The real measurements exhibit delays of the magnetic flux after the magnetic field strength due to the eddy currents, the leakage inductance and, may be, other losses.

The FFT analysis confirmed that magnetic flux waveforms can be considered roughly as harmonic for low excitations, when all the current is negative. The dependence of shift between the exciting current amplitude and the magnetic flux amplitude is in Fig. 8. From practical reasons the measurement number is used instead of the current or flux maximum, but a simple linear relation exists between the parameters.
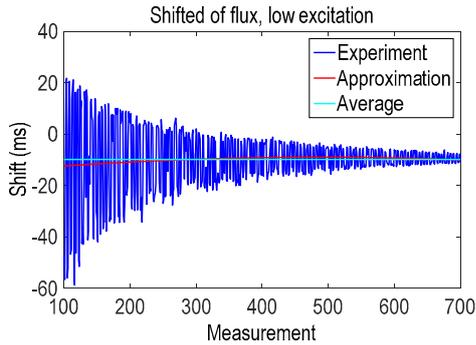

Figure 8. Dependence of shift between the exciting current and the magnetic flux for low excitation.

Fig. 8 confirms that high experimental errors are typical for very low excitation. The shift reaches even impossible positive values. When the excitation increases, the deviations become smaller and acceptable. Also the quasi-periodicity can be found in Fig. 8. However, both the polynomial regression and simple average leads to the time shift of -10 ms, which corresponds to the shift angle of 3.6°.

Since the shift can be determined only for low excitations, we did not made correction for the shift. The second reason is that is not clear what value should be used for synchronization. The average value considers the losses, while the zero value is for no loss medium. The question is discussed later.

The step of the exciting magnetic field strength among neighboring attempts is very small (0.7 A/m approximately); nevertheless, its waveforms are systematically and uniformly arranged according to the excitation. As for the response, the magnetic flux, it is not usually valid, see Fig. 9.
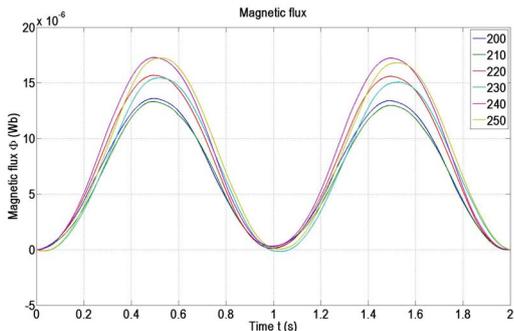

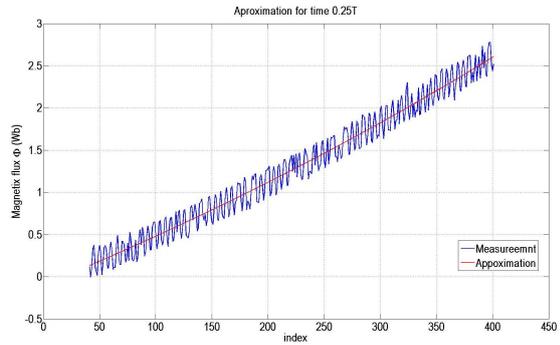Figure 9. Random vertical shift of magnetic flux.

Figure 10. Magnetic flux at given time (quarter of period) for a selected group of measurements.

Although the difference among curves in Fig. 9 is 10 measurements (10 times higher than for the excitation), neither the distance between them is not roughly the same nor is their order natural in agreement with legend. The natural order changes to 210, 200, 230, 220, 250 and 240. Furthermore, the curves in Fig. 9 are connected in pairs.

The last hypothesis is partially confirmed by Fig. 10 that contains magnetic flux for big group of measurements at time $t = 0.25T$, where T is the signal period. At this time the flux increases most rapidly with time, as it can be deduced from Fig. 9. The quasi-oscillations of the magnetic flux with respect to the measurement index are evident in Fig. 10. The mean value of flux is calculated by the polynomial regression

By multiplying the magnetic flux curve as that in Fig. 9 by the coefficients derived from the actual value and the approximating value in Fig. 10, we get the natural order of the curves in Fig. 9. This procedure performs the vertical shift of the flux curves. Unfortunately, the natural and uniform order can be achieved only for the relatively narrow time interval around selected time. For other time the deviations decrease only little and in some cases they can increase.

V. RESULTS

The basic parts of the data improvement are applied in every case before the final waveform processing. The use of the horizontal and vertical shift depends on the user decision, since the improvement can be achieved in one area only and the unwanted changes may appear elsewhere. By the extraction of time from the current and the magnetic flux waveform we get the special minor hysteresis loops. Only their decreasing parts, termed the First Order Reverse Curves (FORC) are important. Only the points of the magnetic field strength with the distance given by the increment ΔH_u between the following measurements are arranged into the Preisach triangle. In our case $\Delta H_u \approx 0.7$ A/m. The 2D surface of magnetic flux density is shown in Fig. 11.

From the point of view of numeric derivation, the most important areas are near the zero excitation, since the flux density changes most rapidly. The flux densities in the selected Preisach triangle rows are shown in Fig. 12, while the flux density in the important selected columns is presented by Fig. 13.
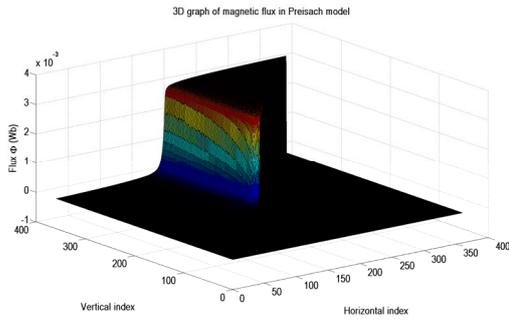
Figure 11. Magnetic flux in the Preisach triangle.

Fig. 12 shows that there are deviations from the expected shape near the curve ends. The waveforms shape along the columns, in Fig. 13, is not smooth which complicates the numeric derivation. The noise in the figure is similar to quasi-periodicity in Fig. 8 for horizontal shift and Fig. 10 for vertical shift in time domain.

In order to get the Preisach weighting function the numeric derivation is made using the Savitzky-Golay filtered derivation by the function *savitzkyGolayFilt*. The smoothing is important for the partial derivation along the columns (with respect to H_u), see Fig. 13. The 2D weighting function is illustrated in Fig. 14 in the form of cuts by horizontal plane. The symmetry to the main diagonal, going from upper left corner to the lower right one is evident. Sharp maximum is near the intersection of the main and the secondary diagonal.

Application of the weighting function in the Preisach model results into the theoretical curve in Fig. 15. The comparison with the experimental curve in Fig. 15 confirms the acceptable agreement from the technical point of view.

VI. DISCUSSION

The experimental curves in Preisach triangle in Fig. 12 and 13 differ from the expected ones. The reason of the deviation is either the experiment inaccuracy or the data processing errors. The unexpected horizontal parts at the end of curves in Fig. 12 are caused by the imperfections of the current source, since the ideal harmonic excitation is not ensured near the zero fields. Explanation is in Fig. 2. The real current cannot reach the harmonic values near the zero crossings. Since the points in the Preisach triangle are for ideal excitation, the flux density cannot be measured for some of them. Last experimental value of flux density is used for them.
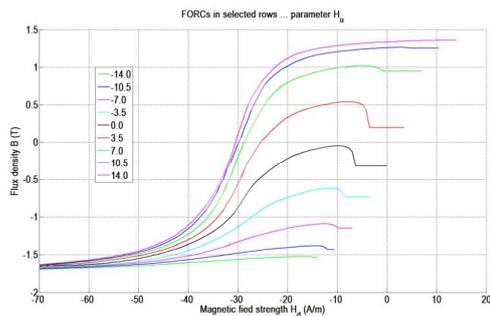

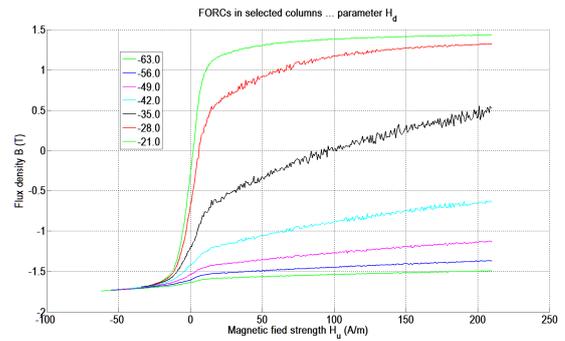Figure 12. Magnetic flux density in the selected rows.

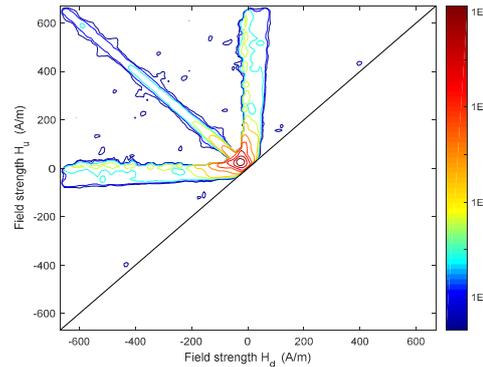Figure 13. Magnetic flux density in selected columns.

Figure 14. Experimental Preisach weighting function for grain oriented steel M130.

The reason of flux density decrease in Fig. 12 can have several causes, first of all experimental ones. It appears only in area close to zero excitation. As the first cause we considered crosstalk between ADC card channels. The use of two cards did not lead to the efficient improvement. The deviation from harmonic excitation in Fig. 2 and pulses of secondary voltage in Fig. 3 can take a place. The solving of this difficult problem is a subject of future investigation. In data processing the end part is constant starting from the curve maximum.

The deviation of curves for columns from smooth shape, the ripples, in Fig. 13 is a consequence of disorder of magnetic flux curves in time domain; see Fig. 9, for instance. The main reason of the disorder may be the experimental inaccuracy, since the neighboring exciting curves differ only little and the accuracy of magnetic measurements is low, in general. The expected accuracy of 1 mT cannot be reached.
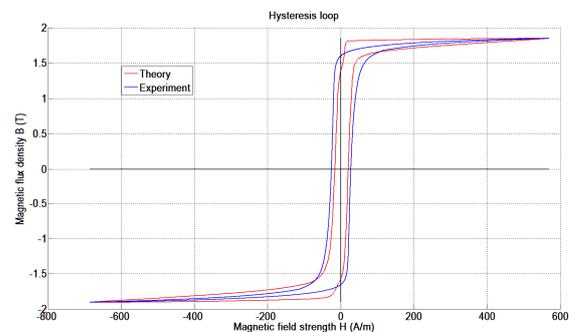

Figure 15. Theoretical and experimental hysteresis loops.

Physical explanation may be the fact that the sample at the start of the measurement is not in perfect saturation. Experimental curve in Fig. 15 exhibits

practically linear decrease of polarization for low excitation. Therefore the starting state of the sample is not defined identically in all successive measurements.

Simulation confirms this assumption partially. Preisach model for starting state in Fig. 16 contains small area of positive momentum. This small area randomly changes from measurement to measurement, since the slope of hysteresis loop is low in this area. Resulting flux density got from this probability model is in Fig. 17. Near the maximum the curve order is preserved, but the distance is not the same. At the starting part the order is 230, 250, 210 and 240. On the other hand the difference between simulation in Fig. 17 and experiment in Fig. 9 indicates that the probability model is more complicated or other effects can take a place.

The FORC in Fig. 12 and 13 has relatively simple shape, which allows to be approximated by simple functions. The function atan of three parameters is a suitable prototype and can be effectively used for high excitations. For low excitation the polynomial regression can be used. Unfortunately, no of the approximations is effective for medium excitation, which is extremely important.

The area inside the hysteresis loop is given by losses that are of different nature. The most important of them are hysteresis losses and eddy current losses. For the study of the hysteresis only the hysteresis losses are important, other losses should be eliminated.

The losses can be estimated by the angle between current and flux, as in Fig. 8 for low excitation. Mean value of shift is 3.6°. The horizontal shift to this value improved the partial loops. If the curves were shifted to zero angles, they became narrower as it is reported in literature [9]. The loss was reduced, unfortunately, we cannot decide if the reduced loss was only the eddy current one. Furthermore, the procedure can be applied only to negative excitation.
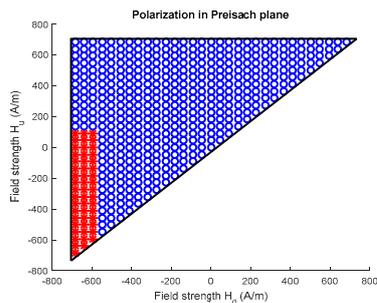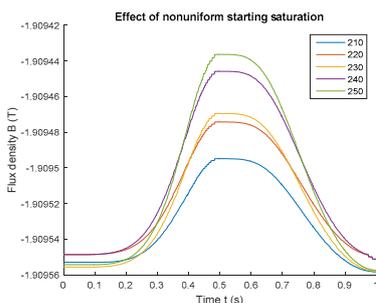
The effect of eddy currents can be studied experimentally by increasing the excitation frequency, while other parameters do not change. The eddy current losses are proportional to the square of frequency. By the losses extrapolation to zero frequency the hysteresis losses can be found in principle. The experiment is in preparation.

VII. CONCLUSIONS

To our knowledge such extended experiment was not used to obtain data for the Preisach model. The agreement with the experiment is acceptable for praxis and is of the same quality as for the estimated analytical weighting function presented in the paper [8]. From the practical point of view the experimental approach is better because can be fully automated. It does not require experienced user.

Modification of Preisach model by inclusion of random effects was studied and can explain some problems. Main improvement is in the experimental area, since the main problem is to ensure the deep saturation of the sample and repeatability of the experiment, mainly reduction of the ripples in Fig. 10 or 13. The simplest way is to repeat experiment under the same conditions and take the average values.

REFERENCES

[1] G. Bertotti, I. Mayergoyz, The science of hysteresis. Vol. 1, 2 and 3. 1st ed., Elsevier, 2006. ISBN 978-0--2-369431-7, Chapter 3.

[2] I. Mayergoyz, Mathematical models of hysteresis and their applications. 1st ed., Elsevier, 2003, ISBN 0-12-480873-5

[3] L. L. Rouve. Th. Waeckerle, A. Kedous-Lebous, "Application of Preisach model to grain oriented steels: Comparison of different characteristizations for the Preisach function p(α, β)," IEEE Trans. on Magnetics, vol. 31. no. 6, pp. 3557-3559, Nov. 1995.

[4] J. Füzi, "Analytical approximation of Preisach distribution functions," IEEE Trans. on Magnetics, vol. 39. no. 3, pp. 1357-1360, May. 2003.

[5] J. Eichler, M. Novak, M. Kosek, Implementation of the first order reversal curve method for identification of weighting function in Preisach model for ferromagnetics, will be published in Proceedings of 11th International Conference ELEKTRO, Strbske Pleso, High Tatras, Slovakia, May 16th-18th, 2016.

[6] S. V. Menon and C. S. Seelamantula, "Robust Savitzky-Golay filters," Digital Signal Processing (DSP) 2014, 19th Intern. Conf. on, Hong Kong, 2014, pp. 688-693.

[7] B. Schettino; C. Duque; P. Silveira, "Current-Transformer saturation detection using Savitzky-Golay filter," in IEEE Transactions on Power Delivery , vol.PP, no.99, pp.1-1.

[8] J. Eichler, M. Kosek and M. Novak, "Two methods of scalar Preisach function identification for grain oriented steel," Applied Electronics (AE), 2015 International Conference on, Pilsen, 2015, pp. 37-40.

[9] M. Patocka, Magnetic effects and circuits in power electronics, measurement technique na high-current electrical engineering. Ecnical university in Brno, VUTIUM, 2011 (in Czech.

Figure 16. Preisach model for initial saturation.

Figure 17. Response of Presiach model of random staring state.